Unlocking the Potential of Halide Perovskites Through Doping
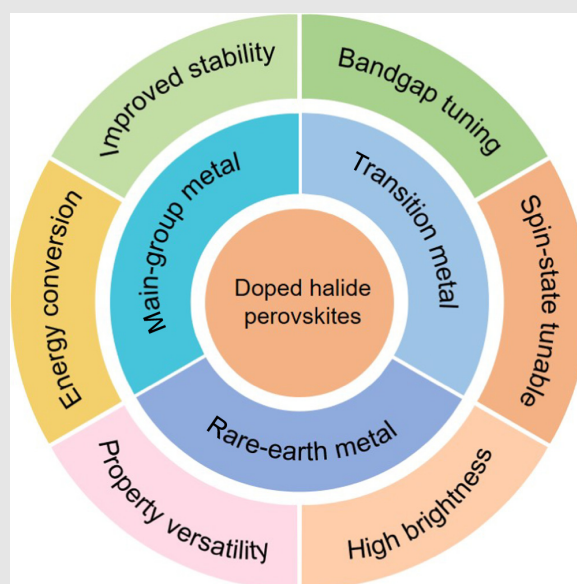
Chenlu He[1], Jian Qiu[1,2], Zhen Mu[1] & Xiaogang Liu[1,2,3]*

[1]Department of Chemistry, National University of Singapore, Singapore 117549, [2]Joint School of National University of Singapore and Tianjin University, International Campus of Tianjin University, Binhai New City, Fuzhou 350207, [3]Institute of Materials Research and Engineering, Agency for Science, Technology and Research, Singapore 138634

*Corresponding author: chmlx@nus.edu.sg

Halide perovskites have become a hot topic in materials research due to their potential applications in a variety of fields, from optoelectronic and thermoelectric devices to solar cells. Doping of halide perovskites can be achieved by introducing different types of dopants, such as metal cations, anions, and organic molecules, leading to increased stability and improved optoelectronic properties. Moreover, doping can introduce new functionalities, such as increased spin lifetime and thermal stability. These features make doped halide perovskites a highly promising candidate for optoelectronic applications. In this mini-review, we highlight the latest advances in ion-doped halide perovskites and their immense potential for various applications.
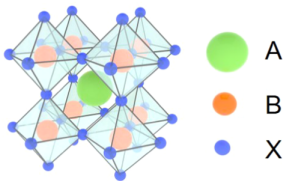
Introduction

Halide perovskites are a broad class of semiconductor materials with the chemical formula ABX_3, where A is a monovalent inorganic or organic cation (e.g., Cs^+ or $CH_3NH_3^+$), B is a divalent metal cation (e.g., Pb^{2+}), and X is a halide anion (Cl^-, Br^-, I^-).[1,2] Low-dimensional derivatives of this three-dimensional (3D) crystal structure have also been engineered, in which the A site has been partially or fully replaced by a larger volume of organic

cations, enabling layered (two-dimensional), chained (one-dimensional), and mixed-dimensional perovskites.[3,4] With appropriate selection of constituents, halide perovskites feature an immense degree of tunability of semiconducting properties, such as a tunable bandgap, narrow spectral width, long charge carrier mobility, and strong optical absorption, making them an ideal candidate for light-emitting diodes (LEDs), photodetectors, photovoltaics, and other optoelectronic fields.[5,6] This compositional engineering has led to major advances in

Figure 1 | *Types of doping ions investigated in halide perovskites. Green, yellow, and blue represent the type of ion doping on the A-site, B-site, and X-site, respectively. Doping in halide perovskites can be achieved by different mechanisms, including substitutional, interstitial, and surface adsorption doping. Substitutional doping involves replacing one or more halide ions with a foreign ion, whereas interstitial doping involves introducing a foreign ion into the perovskite's interstitial sites. Surface adsorption doping entails deposition of a foreign molecule or atom on a crystal surface.*

the photophysical performance of perovskite-based devices in terms of stability and efficiency.[7] However, perovskites still suffer from several drawbacks that need to be circumvented before this material can find long-term application. For example, the intrinsic crystal phase transition of perovskite-based devices during operation and the poor stability when exposed to moisture, high temperature, and ultraviolet light.[8] Moreover, device performance still needs to be improved, and integrating perovskite optoelectronics with versatile functionalities remains a challenge.

Doping, a process in which impurity ions are intentionally introduced into a target host, is an effective method to tune the semiconducting properties of halide perovskites without excessively changing their crystal structure and basic characteristics.[9] Generally, a suitable doping technique for perovskites can stabilize crystal structures, reduce defect density, or tune luminescence properties.[10] This simple strategy can optimize the optoelectronic properties of perovskites or potentially discover novel properties beneficial to technological applications.[11] To this end, a variety of ions, including cations of main-group metals (e.g., Na$^+$), transition metals (e.g., Mn^{2+}), and rare-earth metals (e.g., Yb^{3+}), have been doped into perovskite matrices, imparting a wide variety of exotic properties to this prominent material.[12]

In this mini-review, we discuss recent developments in ion-doped halide perovskites, focusing on various methods used to enhance the photophysical properties of perovskites, such as tuning their optical and spin-related properties, improving their stability and quantum yields. We also address outstanding challenges in this field and preview possible avenues for future research (Figure 1).

Bandgap Tuning

The tunable crystal structure of perovskites (ABX$_3$) enables precise control of the bandgap through doping at the A, B, and X sites, resulting in high fluorescence quantum yields and emission in the visible and near-infrared regions. Specifically, doping at the A site can alter the bandgap and shift the emission wavelength (Figure 2a).[13,18,19] The size and charge of the ion occupying the A site play a crucial roles in this process because they can affect the crystal lattice parameters and symmetry, leading to changes in the optical and electronic properties of the material. For example, Sun et al.[20] showed that Cs$^+$ doping can reduce the lattice constant and enlarge the bandgap in MAPbBr$_3$ perovskite nanocrystals. Similarly, Chen et al.[21] achieved tunable luminescence over a broad spectrum by replacing Cs$^+$ with FA$^+$ in perovskite
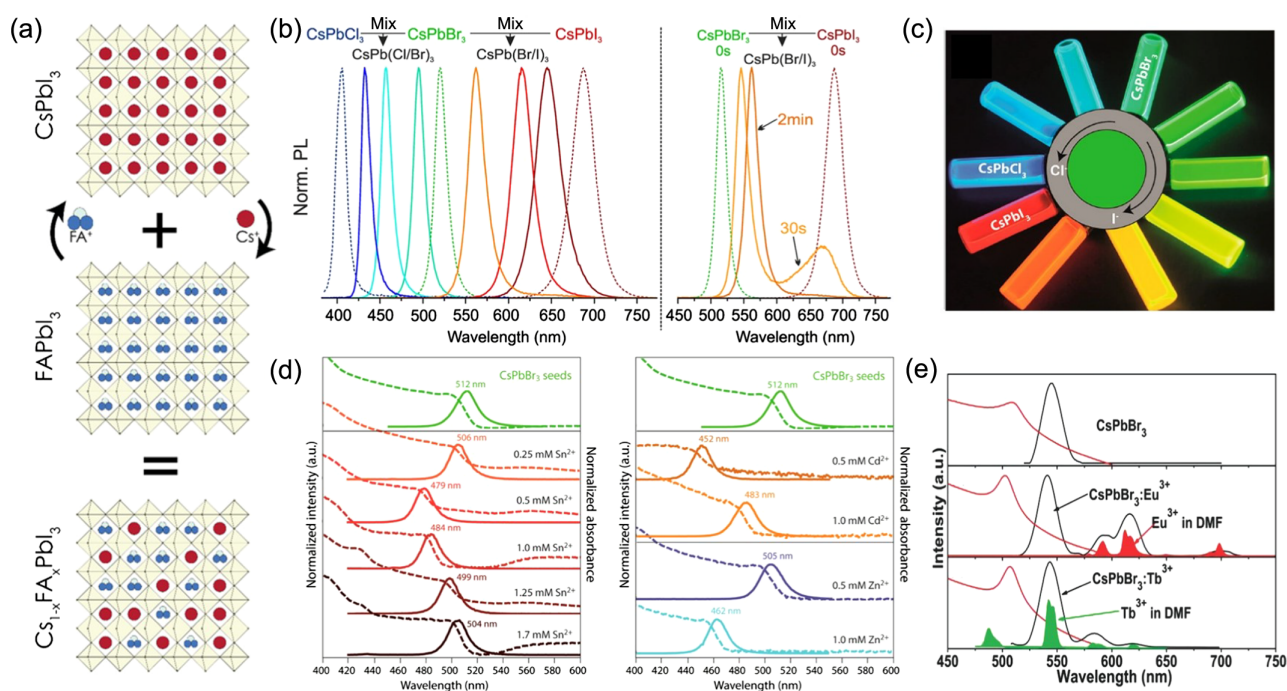
Figure 2 | (a) Schematic showing the cross-exchange of Cs^+ and FA^+ ions between $CsPbI_3$ and $FAPbI_3$ perovskite. Reprinted with permission from ref 13. Copyright 2018 American Chemical Society. (b) PL spectra of samples obtained by mixing $CsPbBr_3$ with either $CsPbCl_3$ or $CsPbI_3$ at various ratios. Reprinted with permission from ref 14. Copyright 2015 American Chemical Society. (c) Picture of the different $CsPbX_3$ solutions obtained by anion exchange under a UV lamp. Reprinted with permission from ref 15. Copyright 2018 American Chemical Society. (d) PL and absorption spectra of $CsPbBr_3$ and after reacting with $SnBr_2$ and $ZnBr_2$ at different concentrations. Reprinted with permission from ref 16. Copyright 2017 American Chemical Society. (e) The absorption and PL spectra of $CsPbBr_3$; $CsPbBr_3:Eu^{3+}$; and $CsPbBr_3:Tb^{3+}$. Reprinted with permission from ref 17. Copyright 2018 Wiley-VCH.

quantum dots. Etgar et al.[22] also demonstrated tunable emission in the 395–525 nm range by Rb^+ doping at the A site. Overall, A-site doping slightly alters the bandgap by changing the size of the impurities, which impacts the lengths and angles of $[PbX_6]^{4-}$ octahedra.

Compared with A-site doping, X-site doping, which adjusts the ratio of halogen atoms in perovskites, offers a more convenient way to achieve tunable luminescence across the entire visible range. This is due to the combined influence of halogen atoms and Pb^{2+} on the structure of the valence band (Figure 2c).[15,23,24] Kovalenko et al.[14] reported that tuning the ratio of halogen atoms (Cl, Br, I) in perovskite crystals by rapid internanocrystal anion exchange can readily tune the luminescence wavelength (Figure 2b). According to Zhao and colleagues,[25] introduction of SCN^- dopants in $CsPbBr_3$ perovskite nanocrystals causes a blue-shift in luminescence. This effect is attributed to the disorder created within the crystal lattice, leading to the broadening of the bandgap. Additionally, the mixed halide strategy exhibits exceptional stability and high fluorescence quantum yield.[26]

B-site doping can significantly affect the bandgap and the channel for radiative recombination. When Pb^{2+} ions are partially substituted, the lattice can expand or contract, leading to a red- or blue-shift in the spectrum. The bandgap can be widened by doping halide perovskites with ions that are smaller than Pb^{2+}. This widening effect has the potential to produce luminescence in the blue range. For example, de Mello Donega et al.[16] synthesized $CsPb_{1-x}M_xBr_3$ (M= Sn^{2+}, Cd^{2+}, and Zn^{2+}) nanocrystals through partial cation exchange, resulting in a blue-shift in their spectra (Figure 2d). Successful doping of perovskites with Sr^{2+}, Ni^{2+}, and Mn^{2+} has been reported.[27,28] Doping with Sr^{2+} leads to a widening of the bandgap, while doping with Ni^{2+} causes a red-shift in the spectrum by improving the lattice order.[29] Doping with Mn^{2+} enables multicolor luminescence by creating new luminescent centers that coexist with the perovskite.[30,31] In addition, rare earth ions (Eu^{3+}, Ce^{3+}, Sm^{3+}, Tb^{3+}, Dy^{3+}, Er^{3+}, and Yb^{3+}) are highly effective dopants at the B-site of perovskites as they possess a rich energy-level structure that can introduce new luminescence levels to the radiative recombination of perovskites (Figure 2e).[17,32,33] Exciton energy can be transferred to rare-earth energy levels and then relaxed nonradiatively to the emission level, resulting in remarkable multipeak emissions. This process can be utilized to emit white light.
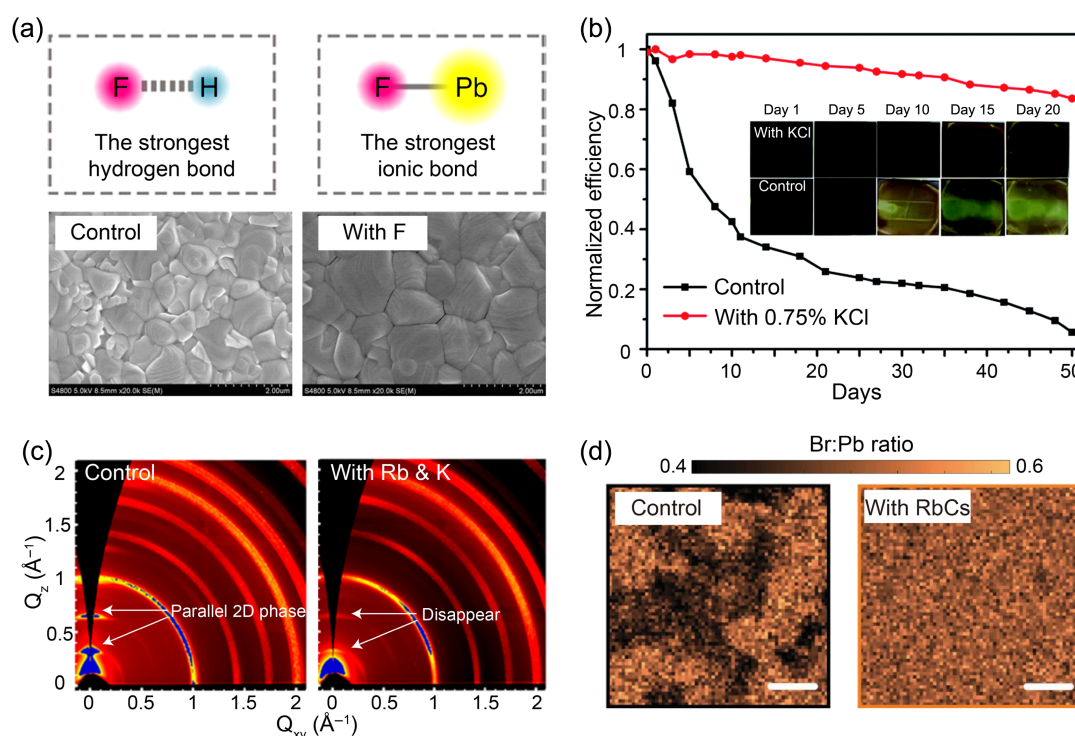
Figure 3 | *(a) Scanning electron microscopy (SEM) images of the NaF-doped perovskite film and the control. Reprinted with permission from ref 35. Copyright 2019 Spring Nature. (b) Efficiency stability of the KCl-doped thin-film perovskite solar cells and the control. The inset pictures are real photos of control and KCl doped perovskite films stored in air. Reprinted with permission from ref 36. Copyright 2016 Royal Society of Chemistry. (c) 2D GIWAXS patterns of the Rb and K codoped 2D/3D mixed perovskite film and the control. Reprinted with permission from ref 37. Copyright 2020 American Chemical Society. (d) X-ray fluorescence mapping of the Rb and Cs codoped I/Br mixed perovskite film and the control, indicating the uniform distribution of halogens after doping. Scale bar is 2 μm. Reprinted with permission from ref 38. Copyright 2019 American Association for the Advancement of Science.*

Morphology and Crystallinity Optimization

Poor morphology of perovskite films, including the presence of pinholes and voids, can facilitate water and oxygen penetration, leading to perovskite decomposition and reduced stability in the corresponding optoelectronics. Therefore, high-quality perovskite films with full surface coverage are essential for stable optoelectronics. To obtain high-quality perovskite films, the kinetics of crystal growth must be controlled.[34] For instance, F^- ions, which have larger electronegativity and a smaller ionic radius compared to other halogens, exhibit the strongest hydrogen bonding with organic ammonium cations (e.g., $CH_3NH_3^+$) and the strongest ionic bonding with metal cations (e.g., Pb^{2+}, Figure 3a).[35] The strong chemical interactions between doped F^- and perovskite precursors can effectively delay the crystallization rate, resulting in high-quality perovskite films with full surface coverage and large grain size. Zn^{2+} can also be used as a dopant in perovskite precursors to replace Pb^{2+} ions,

which can affect the crystallization process and lead to the formation of perovskite films with good morphology and enhanced stability. This is because Zn^{2+} ions are stronger Lewis acids than Pb^{2+} ions.[39] Additionally, alkali metal ions such as Na^+, K^+, and Rb^+, which have high chemical activity, can also strongly interact with perovskite precursors, and regulate the kinetics of crystal growth, resulting in stable and high-quality perovskite films and optoelectronic devices with long-term operational stability (Figure 3b).[36]

Inorganic ions not only affect film morphology but also play a crucial role in adjusting the crystallinity of perovskite films, including crystal orientation and the distribution of mixed halogens. For example, in 2D/3D mixed perovskites, the parallel-oriented 2D perovskite phases severely affect the uniform expansion of crystal domains and reduce the crystallinity and stability of the films. Codoping with inorganic ions Rb^+ and K^+ can help to resolve this problem. The 2D grazing-incidence wide-angle X-ray scattering (GIWAXS) patterns show that films with Rb^+ and K^+ exhibit less parallel-oriented 2D perovskite phases, whereas undoped films still exhibit
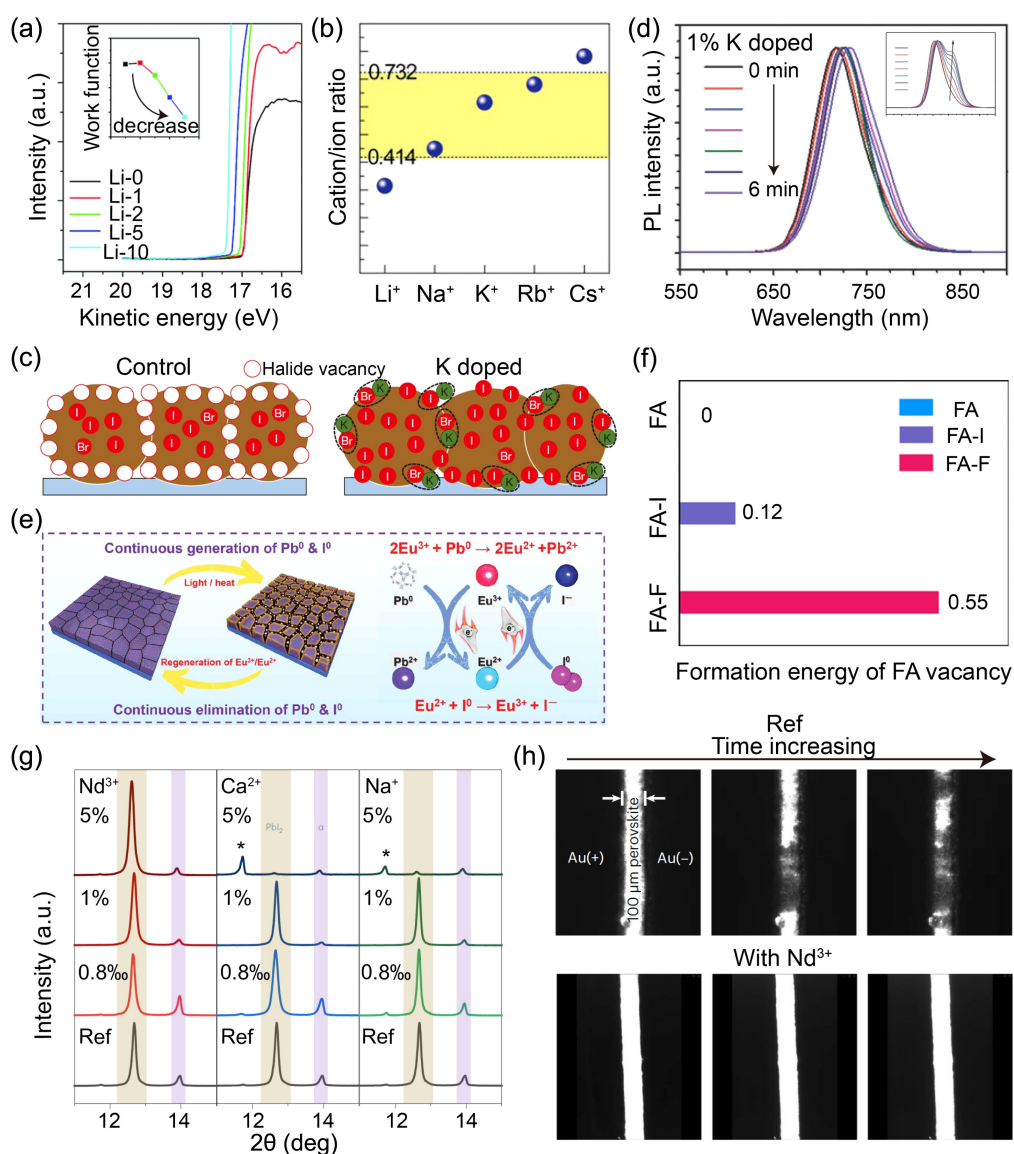
Figure 4 | *(a) Ultraviolet photoelectron spectroscopy (UPS) of Li^+-doped perovskite films. The inset shows the work function of the perovskite versus the amount of doped Li^+. Reprinted with permission from ref 42. Copyright 2018 Wiley-VCH. (b) Cation/anion ratio between doped metal ions and halogen ions in perovskites. Reprinted with permission from ref 43. Copyright 2018 American Chemical Society. (c) Schematic of the interaction of doped ions with halogens, resulting in suppression of vacancies. Reprinted with permission from ref 44. Copyright 2018 Spring Nature. (d) PL stability of K-doped perovskite films. The inset shows the PL stability of control samples. Reprinted with permission from ref 45. Copyright 2018 Wiley-VCH. (e) The mechanism of rare-earth metal ions (Eu) to suppress I^0 and Pb^0 defects in perovskites. Reprinted with permission from ref 46. Copyright 2019 American Association for the Advancement of Science. (f) Calculated formation energy of formamidine (FA) vacancies in perovskites without dopant and with F^- or I^-. Reprinted with permission from ref 35. Copyright 2019 Spring Nature. (g) Comparison of different perovskite phases using X-ray diffraction (XRD) patterns of perovskite films doped with different Nd^{3+}, Ca^{2+}, and Na^+ concentrations. The * represent the non-perovskite δ-phases. (h) In-situ PL images of perovskite films without and with Nd^{3+} under an electric field. Reprinted with permission from ref 47. Copyright 2022 Spring Nature.*

clear 2D phases (Figure 3c).[37] This is likely due to the gradual increase in the size of doped ions caused by cascade doping, which leads to an expansion of crystal distortion and kinetically favored facet orientation.[40] Furthermore, phase separation is a known problem in

halogen mixed perovskites, such as I/Br mixed perovskites, which can result in poor film crystallinity and lowered stability. Doping with inorganic ions can alleviate this issue, as demonstrated by Fenning et al.[38] who systemically explored the effects of different stoichiometric

dopants of Rb^+ and Cs^+ on halogen-phase separation using synchrotron-based nano-X-ray fluorescence and complementary measurements. The results indicate that moderate doping of Cs^+ or codoping of Cs^+ and Rb^+ can effectively prevent I/Br separation (Figure 3d). However, the underlying mechanism of how doping with inorganic ions suppresses the halogen-phase separation remains unknown.

Trap-State Passivation and Ion-Migration Suppression

Halide perovskites are prone to form traps and defects due to the soft nature of their main constituents, leading to ion migration and reduced stability.[41] Doping ions into perovskites can passivate the traps and suppress ion migration, thereby improving the stability of the perovskite. For example, Li^+-doped perovskites can act as n-type donors, reducing the work function of perovskites and providing free charge carriers to fill the oxidized trap states, improving the stability of perovskite devices (Figure 4a).[42] However, the effectiveness of Li^+ in passivating trap states is limited as Li^+ is too small to hinder the migration of I^- ions into interstitial sites. Li^+ ions in perovskite lattices cannot occupy interstitial sites, and this leads to the accumulation of electrons and formation of I-Frenkel defects.[43] On the other hand, K^+ ions have a comparable size and ratio with I^- in perovskites, making them more compatible with interstitial sites (Figure 4b). Therefore, when perovskites are doped with potassium halide salts (e.g., KI), K^+ ions can diffuse uniformly into interstitial sites, effectively preventing the formation of I-Frenkel defects. Furthermore, diffusion of excess K^+ and I^- ions into the film surface or grain boundaries can immobilize halogens and fill halide vacancies, thereby preventing halide migration, alleviating phase separation, and suppressing nonradiative recombination (Figure 4c,d).[44,45]

Rare-earth elements such as Eu have been found to suppress Pb^0 and I^0 defects in perovskites through the use of a Eu^{3+}-Eu^{2+} redox shuttle.[46] This involves the reduction of I^0 to I^- by Eu^{2+}, followed by the formation of Eu^{3+}, which can oxidize Pb^0 to Pb^{2+}, forming a cycle (Figure 4e). This Eu^{3+}-Eu^{2+} redox shuttle has been shown to significantly improve the stability of perovskite devices. Moreover, organic ammonium ions can cause vacancies in perovskite lattices when they volatilize. These doped ions with strong chemical interaction, such as F^-, can anchor ammonium ions through hydrogen bonds and prevent them from escaping, inhibiting the formation of ammonium vacancies.[35] The formation energy of FA^+ vacancies in F^--doped perovskites is higher than that of control and I^--doped perovskites (Figure 4f). Excessive doping can cause deformation of perovskite lattices, resulting in a decrease in stability (Figure 4g).[47] Therefore, low doping with efficient trap passivation and

suppression of ion migration is desirable. Trivalent cations such as Nd^{3+} can effectively suppress ion migration at a low dose of 0.08% (Figure 4h).[48] Unlike Ca^{2+} or Na^+ doping, Nd^{3+} doping has been shown not to form nonperovskite δ-phases even at high doses of 5%, suggesting that Nd^{3+} doping can still effectively suppress δ-phases and promote the formation of the stable black perovskite α-phase (Figure 4g).[48,49] However, the deep mechanism behind this requires further exploration.

The promotion and stabilization of the black perovskite phase in $FAPbI_3$ or $CsPbI_3$ are crucial for achieving high performance and stable single-junction perovskite photovoltaics.[50] The introduction of chloride ions (Cl^-) during the precursor synthesis of $FAPbI_3$ has proven effective in stabilizing the black α-$FAPbI_3$. This stabilization occurs due to the Cl^- ions inducing p orbital localization of I^- ions, which enhances their intensity at the highest occupied molecular orbital state. Consequently, this improves the interaction between I^- and FA^+, leading to the stabilization of the black phase.[51] In the case of $CsPbI_2Br$ perovskite, the successful doping of Eu^{2+} at the atomic level has been observed to enhance the thermodynamic stability of the black phase at room temperature by strengthening the ionic bond.[52,53] Apart from inorganic ions, organic ions such as pyridine-2-carboxylate exhibit strong interaction with perovskites and can suppress the transition from the black perovskite phase to an inactive phase.[54]

Lattice Strain Relaxation

During perovskite growth, lattice strain often occurs due to various factors such as heat, mechanical deformation, and lattice mismatch.[55] This strain has been found to increase defect concentration and nonradiative recombination, which negatively affects perovskite stability.[56,57] In general, perovskites release lattice strain by forming point defects to maintain crystal systems at the lowest energy level (Figure 5). However, these point defects reduce stability. On the contrary, doping ions with a suitable size can support strain relaxation with minimal side effects.[58] There are many candidates for doping ions to release lattice strain, including soft/intermediate Lewis acids (Hg^{2+}, Cd^{2+}, Zn^{2+}) and hard Lewis acids (Ba^{2+}, Sr^{2+}, Ca^{2+}) for the B site, and Lewis bases (Cl^-, Br^-, I^-) for the X site in halide perovskites. It should be noted that unlike crystal tilts caused by local strains, moderate crystal lattice tilts induced by uniformly doped ions can reduce the internal energy of the system, which can stabilize the crystal structure. As with local strains, overdosing of ions can have negative effects such as causing severe lattice tilting, increasing internal energy, and destabilizing crystals. Therefore, it is crucial that the doping of ions in perovskites is performed homogeneously and the appropriate amount is used.
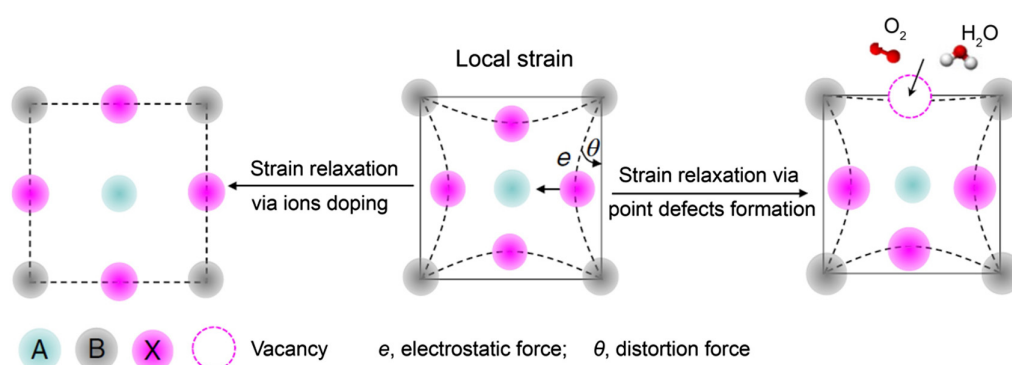
Figure 5 | *Schematic of local strain dynamics. It can be reduced by forming point defects or by doping with suitable ions. Reprinted with permission from ref 58. Copyright 2018 Spring Nature.*

Spin-State Regulation

Lead halide perovskites are promising materials for spin-related applications due to their strong spin-orbital coupling (SOC).[59] This intrinsic property has led to increasing efforts to investigate and tune the spin state of charge carriers in perovskites, making them a strong candidate for optospintronics.[60] This technology combines spin degrees of freedom with photons and charges, resulting in lower power consumption and faster switching times than conventional electronic systems. However, the strong SOC effect also shortens the lifetime of spin states in perovskites to a few picoseconds at room temperature, limiting their spin-related applications. Therefore, it is essential to understand the mechanism of spin decoherence and improve the spin-relaxation time in perovskites.

In recent studies, Wu et al.[61] investigated spin relaxation in $CsPbI_3$ and $CsPbBr_3$ perovskite nanocrystals at room temperature using circularly polarized transient absorption spectroscopy and found that spin lifetime decreases with decreasing size. The spin relaxation was prolonged to ~18 ps by replacing heavy-metal Pb with lighter Sn, which attenuates the SOC effect (Figure 6a).[62] In another study, Beard et al.[63] prolonged the exciton spin relaxation in two-dimensional perovskite single crystals to ~26 ps by changing organic ligand components (Figure 6b). Moreover, Jin et al.[64] explored the influence of Bi doping on the spin-relaxation dynamics of charge carriers in $CsPbBr_3$ nanocrystals (Figure 6c). The spin relaxation in Bi-doped nanocrystals was prolonged to ~24.6 ps by adjusting the Bi doping amount, which introduced ultrafast hole trapping (~0.13 ps) and disrupted electron–hole exchange.

Doping transition metals in the perovskite lattice can improve the performance of photocatalysts by tuning the spin-relaxation process. Chen et al.[65] enhanced photocatalytic CO_2 reduction efficiency by doping Mn^{2+} into $CsPbBr_3$ nanoplates, which resulted in increased spin-polarized carriers under an external magnetic field, prolonged carrier lifetime, and suppressed charge recombination (Figure 6d). Despite notable progress, current methods for tuning the spin state in perovskites through doping remain limited, and further exploration is needed to unlock the potential spin-related applications of perovskites, including 3D display and circular polarized emission from chiral perovskites at room temperature.

Challenges and Perspectives

Although significant progress has been made in perovskite materials, there is still limited understanding of doped halide perovskites, including synthesis and doping methods, structure-performance relationships, and intrinsic mechanisms for optoelectronic properties.[66,67]

A major challenge is the lack of complete structural information about the doped ions in halide perovskites, including the crystallographic sites occupied by dopants and the distribution of ions.[68] This is because perovskites are composed of a variety of components, including the perovskite lattice, dopants, and inorganic and organic molecules that form a complex three-dimensional network. Precise characterization techniques, such as steady-state absorption and emission spectroscopy and X-ray photoelectron spectroscopy, have provided insight into ion doping.[69-71] However, more advanced techniques such as time-of-flight secondary ion mass spectrometry are needed to gain a comprehensive understanding of these complex systems. These techniques offer improved means of observing doping information and represent a novel viewpoint for further investigation of the success of ion doping in perovskites.[72,73]

Another challenge is that current dopant engineering for perovskites has primarily focused on three-dimensional structures, but there is potential for dopant-assisted performance tuning in low-dimensional perovskites. Two-dimensional halide perovskites, for example, offer
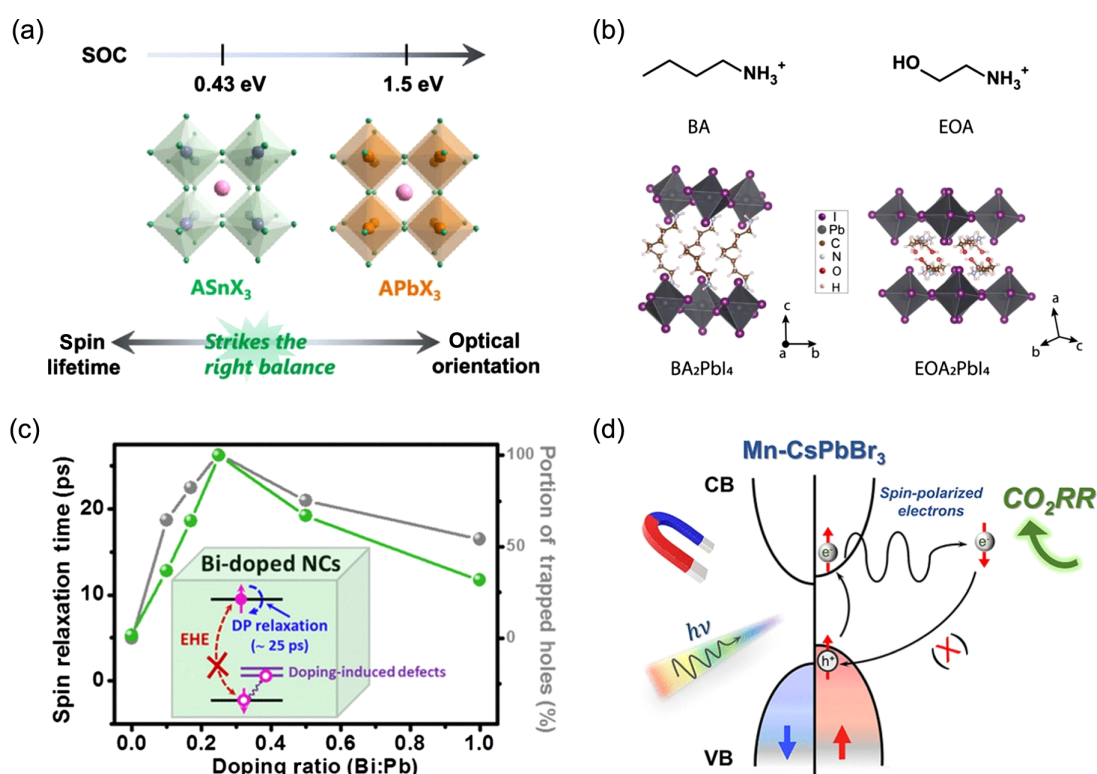
Figure 6 | *(a) CsSnBr₃ nanocrystals strike the balance between optical orientation and spin relaxation through appropriate SOC strength. (b) Chemical and crystal structures of organic ammonium cations and corresponding hybrid two-dimensional perovskites. (c) Spin-relaxation time in Bi-doped CsPbBr₃ nanocrystals as a function of the Bi-to-Pb ratio at room temperature. (d) Schematic of the electron spin-polarization-inducing longer lifetime of photo-excited charge carriers in Mn-doped CsPbBr₃ nanoplates under an external magnetic field, boosting the photocatalytic CO₂ reduction efficiency. Reprinted with permission from refs 62 and 63. Copyright 2021 American Chemical Society; refs 64 and 65. Copyright 2022 American Chemical Society.*

opportunities to research the interaction between optically, electronically, and magnetically active dopants and quantum confinement effects. Meanwhile, low-dimensional chiral perovskites, obtained by inserting chiral organic molecules into three-dimensional matrices, have potential for chiroptoelectronics because they can manipulate the spin of photons/electrons without requiring an external magnetic component. This field has attracted a wide range of researchers with expertise in hybrid perovskites, chirality, and spintronics. However, the dissymmetry factors (g_{abs}) of chiral perovskites are very low ($<10^{-2}$), and the mechanisms of chirality transfer from the molecular level to the nanoscale remain unclear.[74] Moreover, the properties of circularly polarized emission from chiral perovskites depend on temperature. At low temperatures, the emission is usually circularly polarized, while at room temperature it is almost unpolarized.[75] Therefore, researchers should focus on designing and integrating novel chiral dopants into perovskites that introduce greater structural asymmetry. This can potentially improve the enantioselectivity of circularly polarized emission from chiral perovskites at room temperature, which is desirable

for various applications and can advance the field of chiroptoelectronics, ferroelectrics, and spintronics.

Doped perovskite scintillators possess high light output, excellent energy resolution, and fast response time, rendering them ideal for radiation detection, environmental monitoring, and medical imaging.[76,77] In X-ray computed tomography, for example, these scintillators can convert X-rays into visible light that can be detected and used to generate detailed images of internal structures within the human body. The use of doped perovskite scintillators with high light yield and energy resolution provides high-quality images while minimizing patients' radiation exposure.[78] Moreover, these scintillators can be integrated into wearable or implantable dosimetry devices for real-time monitoring of radiation exposure during radiotherapy.[79,80] Current research in this field continues to explore the fundamental properties and performance of doped perovskite scintillators, as well as their integration into advanced technologies for diverse applications. We believe that further developments and optimization will enable multifunctional perovskite scintillators to revolutionize the field.

Rare earth (RE³⁺)-doped perovskites have received significant attention due to their unique structural and optical properties.[81] These positively charged RE^{3+} ions can replace either the A or B cation in the perovskite structure, depending on their size. By doping halide perovskites with RE^{3+}, it is possible to generate materials with exceptional structural and optical properties that can be used for a range of applications. They exhibit high photoluminescence (PL) quantum yield, narrow emission linewidth, and long luminescence lifetime, making them attractive for solid-state lighting and sensing applications. Moreover, RE^{3+}-doped perovskites can exhibit upconversion luminescence, converting low-energy photons into higher-energy photons, which is beneficial for enhancing light output in solar cells. Furthermore, RE^{3+}-doped perovskites exhibit improved thermal stability, making them suitable for high-temperature applications. This enhanced stability contributes to the durability and longevity of devices and systems incorporating these materials.

Despite their many useful properties, RE^{3+}-doped perovskites face challenges, particularly regarding stability, as they can degrade over time due to moisture and oxygen exposure. Additionally, their synthesis and doping processes can be difficult. Therefore, further research is needed to enhance stability, improve synthesis methods, and develop practical integration strategies. However, the continued advances in materials science suggest that RE^{3+}-doped perovskites hold great potential for revolutionizing various industries and technologies. Notably, they offer a sustainable alternative to traditional LEDs, with high PL quantum yield and tunable emission wavelengths, making them suitable for efficient and color-tunable lighting applications.[82]

Conclusions

Halide perovskites doped with various elements provide a fascinating and promising platform for optoelectronic applications. The combination of their remarkable optical, electrical, and structural properties, as well as their low cost and ease of fabrication, make them an ideal candidate for many future applications. Further research should focus on understanding the effects of doping, characterizing the precise distribution of doped ions, and optimizing the performance of perovskites. We believe that doped halide perovskites will have a significant impact on the future of materials science.

Conflicts of Interest

The authors declare no competing financial interests.

Acknowledgments

References

1. Chen, S.; Yin, H.; Liu, P.; Wang, Y.; Zhao, H. Stabilization and Performance Enhancement Strategies for Halide Perovskite Photocatalysts. *Adv. Mater.* **2023**, *35*, 2203836.

2. Lee, J.-W.; Tan, S.; Seok, S. I.; Yang, Y.; Park, N.-G. Rethinking the A Cation in Halide Perovskites. *Science* **2022**, *375*, 835.

3. Hong, K.; Van Le, Q.; Kim, S. Y.; Jang, H. W. Low-Dimensional Halide Perovskites: Review and Issues. *J. Mater. Chem. C* **2018**, *6*, 2189.

4. Wang, G.; Mei, S.; Liao, J.; Wang, W.; Tang, Y.; Zhang, Q.; Tang, Z.; Wu, B.; Xing, G. Advances of Nonlinear Photonics in Low-Dimensional Halide Perovskites. *Small* **2021**, *17*, 2100809.

5. Cho, Y.; Jung, H. R.; Jo, W. Halide Perovskite Single Crystals: Growth, Characterization, and Stability for Optoelectronic Applications. *Nanoscale* **2022**, *14*, 9248.

6. Chen, Q.; Wu, J.; Ou, X.; Huang, B.; Almutlaq, J.; Zhumekenov, A. A.; Guan, X.; Han, S.; Liang, L.; Yi, Z.; Li, J.; Xie, X.; Wang, Y.; Li, Y.; Fan, D.; Teh, D. B. L.; All, A. H.; Mohammed, O. F.; Bakr, O. M.; Wu, T.; Bettinelli, M.; Yang, H.; Huang, W.; Liu, X. All-Inorganic Perovskite Nanocrystal Scintillators. *Nature* **2018**, *561*, 88.

7. Otero-Martínez, C.; Ye, J.; Sung, J.; Pastoriza-Santos, I.; Pérez-Juste, J.; Xia, Z.; Rao, A.; Hoye, R. L.; Polavarapu, L. Colloidal Metal-Halide Perovskite Nanoplatelets: Thickness-Controlled Synthesis, Properties, and Application in Light-Emitting Diodes. *Adv. Mater.* **2022**, *34*, 2107105.

8. Chen, W.; Zhou, M.; Liu, Y.; Yu, X.; Pi, C.; Yang, Z.; Zhang, H.; Liu, Z.; Wang, T.; Qiu, J.; Yu, S. F.; Yang, (Michael) Y.; Xu, X. All-Inorganic Perovskite Polymer–Ceramics for Flexible and Refreshable X-Ray Imaging. *Adv. Funct. Mater.* **2022**, *32*, 2107424.

9. Kachhap, S.; Singh, S.; Singh, A. K.; Singh, S. K. Lanthanide-Doped Inorganic Halide Perovskites (CsPbX₃): Novel Properties and Emerging Applications. *J. Mater. Chem. C* **2022**, *10*, 3647.

10. Zhang, X.; Li, L.; Sun, Z.; Luo, J. Rational Chemical Doping of Metal Halide Perovskites. *Chem. Soc. Rev.* **2019**, *48*, 517.

11. Li, C.; Wang, A.; Xie, L.; Deng, X.; Liao, K.; Yang, J.-a.; Li, T.; Hao, F. Emerging Alkali Metal Ion (Li⁺, Na⁺, K⁺, and Rb⁺) Doped Perovskite Films for Efficient Solar Cells: Recent Advances and Prospects. *J. Mater. Chem. A* **2019**, *7*, 24150.

12. Zhou, Y.; Chen, J.; Bakr, O. M.; Sun, H.-T. Metal-Doped Lead Halide Perovskites: Synthesis, Properties, and Optoelectronic Applications. *Chem. Mater.* **2018**, *30*, 6589.

13. Hazarika, A.; Zhao, Q.; Gaulding, E. A.; Christians, J. A.; Dou, B.; Marshall, A. R.; Moot, T.; Berry, J. J.; Johnson, J. C.; Luther, J. M. Perovskite Quantum Dot Photovoltaic Materials

Beyond the Reach of Thin Films: Full-Range Tuning of A-Site Cation Composition. *ACS Nano* **2018**, *12*, 10327.

14. Nedelcu, G.; Protesescu, L.; Yakunin, S.; Bodnarchuk, M. I.; Grotevent, M. J.; Kovalenko, M. V. Fast Anion-Exchange in Highly Luminescent Nanocrystals of Cesium Lead Halide Perovskites (CsPbX$_3$, X= Cl, Br, I). *Nano Lett.* **2015**, *15*, 5635.

15. Imran, M.; Caligiuri, V.; Wang, M.; Goldoni, L.; Prato, M.; Krahne, R.; De Trizio, L.; Manna, L. Benzoyl Halides as Alternative Precursors for the Colloidal Synthesis of Lead-Based Halide Perovskite Nanocrystals. *J. Am. Chem. Soc.* **2018**, *140*, 2656.

16. Van der Stam, W.; Geuchies, J. J.; Altantzis, T.; Van Den Bos, K. H.; Meeldijk, J. D.; Van Aert, S.; Bals, S.; Vanmaekelbergh, D.; de Mello Donega, C. Highly Emissive Divalent-Ion-Doped Colloidal CsPb$_{1-x}$M$_x$Br$_3$ Perovskite Nanocrystals Through Cation Exchange. *J. Am. Chem. Soc.* **2017**, *139*, 4087.

17. Hu, Q.; Li, Z.; Tan, Z.; Song, H.; Ge, C.; Niu, G.; Han, J.; Tang, J. Rare Earth Ion-Doped CsPbBr$_3$ Nanocrystals. *Adv. Opt. Mater.* **2018**, *6*, 1700864.

18. Shi, Y.; Xi, J.; Lei, T.; Yuan, F.; Dai, J.; Ran, C.; Dong, H.; Jiao, B.; Hou, X.; Wu, Z. Rubidium Doping for Enhanced Performance of Highly Efficient Formamidinium-Based Perovskite Light-Emitting Diodes. *ACS Appl. Mater. Interfaces* **2018**, *10*, 9849.

19. Song, J.; Li, J.; Xu, L.; Li, J.; Zhang, F.; Han, B.; Shan, Q.; Zeng, H. Room-Temperature Triple-Ligand Surface Engineering Synergistically Boosts Ink Stability, Recombination Dynamics, and Charge Injection Toward EQE-11.6% Perovskite QLEDs. *Adv. Mater.* **2018**, *30*, 1800764.

20. Xu, B.; Wang, W.; Zhang, X.; Cao, W.; Wu, D.; Liu, S.; Dai, H.; Chen, S.; Wang, K.; Sun, X. Bright and Efficient Light-Emitting Diodes Based on MA/Cs Double Cation Perovskite Nanocrystals. *J. Mater. Chem. C* **2017**, *5*, 6123.

21. Chen, D.; Chen, X.; Wan, Z.; Fang, G. Full-Spectral Fine-Tuning Visible Emissions from Cation Hybrid Cs$_{1-m}$FA$_m$PbX$_3$ (X= Cl, Br, and I, 0≤ m≤ 1) Quantum Dots. *ACS Appl. Mater. Interfaces* **2017**, *9*, 20671.

22. Amgar, D.; Binyamin, T.; Uvarov, V.; Etgar, L. Near Ultra-Violet to Mid-Visible Band Gap Tuning of Mixed Cation Rb$_x$Cs$_{1-x}$PbX$_3$ (X= Cl or Br) Perovskite Nanoparticles. *Nanoscale* **2018**, *10*, 6060.

23. Akkerman, Q. A.; D'Innocenzo, V.; Accornero, S.; Scarpellini, A.; Petrozza, A.; Prato, M.; Manna, L. Tuning the Optical Properties of Cesium Lead Halide Perovskite Nanocrystals by Anion Exchange Reactions. *J. Am. Chem. Soc.* **2015**, *137*, 10276.

24. Zhang, D.; Yang, Y.; Bekenstein, Y.; Yu, Y.; Gibson, N. A.; Wong, A. B.; Eaton, S. W.; Kornienko, N.; Kong, Q.; Lai, M.; Alivisatos, A. P.; Leone, S. R.; Yang, P. Synthesis of Composition Tunable and Highly Luminescent Cesium Lead Halide Nanowires Through Anion-Exchange Reactions. *J. Am. Chem. Soc.* **2016**, *138*, 7236.

25. Lou, Y.; Niu, Y.; Yang, D.; Xu, Q.; Hu, Y.; Shen, Y.; Ming, J.; Chen, J.; Zhang, L.; Zhao, Y. Rod-Shaped Thiocyanate-Induced Abnormal Band Gap Broadening in SCN$^-$ Doped CsPbBr$_3$ Perovskite Nanocrystals. *Nano Res.* **2018**, *11*, 2715.

26. Levchuk, I.; Osvet, A.; Tang, X.; Brandl, M.; Perea, J. D.; Hoegl, F.; Matt, G. J.; Hock, R.; Batentschuk, M.; Brabec, C. J. Brightly Luminescent and Color-Tunable Formamidinium Lead Halide Perovskite FAPbX$_3$ (X= Cl, Br, I) Colloidal Nanocrystals. *Nano Lett.* **2017**, *17*, 2765.

27. Lau, C. F. J.; Zhang, M.; Deng, X.; Zheng, J.; Bing, J.; Ma, Q.; Kim, J.; Hu, L.; Green, M. A.; Huang, S.; Ho-Baillie, H. Strontium-Doped Low-Temperature-Processed CsPbI$_2$Br Perovskite Solar Cells. *ACS Energy Lett.* **2017**, *2*, 2319.

28. Lu, M.; Zhang, X.; Zhang, Y.; Guo, J.; Shen, X.; Yu, W. W.; Rogach, A. L. Simultaneous Strontium Doping and Chlorine Surface Passivation Improve Luminescence Intensity and Stability of CsPbI$_3$ Nanocrystals Enabling Efficient Light-Emitting Devices. *Adv. Mater.* **2018**, *30*, 1804691.

29. Yong, Z.-J.; Guo, S.-Q.; Ma, J.-P.; Zhang, J.-Y.; Li, Z.-Y.; Chen, Y.-M.; Zhang, B.-B.; Zhou, Y.; Shu, J.; Gu, J.-L.; Zheng, L.-R.; Bakr, O. M.; Sun, H.-T. Doping-Enhanced Short-Range Order of Perovskite Nanocrystals for Near-Unity Violet Luminescence Quantum Yield. *J. Am. Chem. Soc.* **2018**, *140*, 9942.

30. De, A.; Mondal, N.; Samanta, A. Luminescence Tuning and Exciton Dynamics of Mn-Doped CsPbCl$_3$ Nanocrystals. *Nanoscale* **2017**, *9*, 16722.

31. Pan, G.; Bai, X.; Xu, W.; Chen, X.; Zhou, D.; Zhu, J.; Shao, H.; Zhai, Y.; Dong, B.; Xu, L.; Song, H. Impurity Ions Codoped Cesium Lead Halide Perovskite Nanocrystals with Bright White Light Emission Toward Ultraviolet–White Light-Emitting Diode. *ACS Appl. Mater. Interfaces* **2018**, *10*, 39040.

32. Pan, G.; Bai, X.; Yang, D.; Chen, X.; Jing, P.; Qu, S.; Zhang, L.; Zhou, D.; Zhu, J.; Xu, W.; Dong, B.; Song, H. Doping Lanthanide into Perovskite Nanocrystals: Highly Improved and Expanded Optical Properties. *Nano Lett.* **2017**, *17*, 8005.

33. Chen, J.; Guo, Y.; Chen, B.; Zheng, W.; Wang, F. Ultrafast and Multicolor Luminescence Switching in a Lanthanide-Based Hydrochromic Perovskite. *J. Am. Chem. Soc.* **2022**, *144*, 22295.

34. Liu, C.; Cheng, Y.-B.; Ge, Z. Understanding of Perovskite Crystal Growth and Film Formation in Scalable Deposition Processes. *Chem. Soc. Rev.* **2020**, *49*, 1653.

35. Li, N.; Tao, S.; Chen, Y.; Niu, X.; Onwudinanti, C. K.; Hu, C.; Qiu, Z.; Xu, Z.; Zheng, G.; Wang, L.; Zhang, Y.; Li, L.; Liu, H.; Lun, Y.; Hong, J.; Wang, X.; Liu, Y.; Xie, H.; Gao, Y.; Bai, Y.; Yang, S.; Brocks, G.; Chen, Q.; Zhou, H. Cation and Anion Immobilization Through Chemical Bonding Enhancement with Fluorides for Stable Halide Perovskite Solar Cells. *Nat. Energy* **2019**, *4*, 408.

36. Boopathi, K. M.; Mohan, R.; Huang, T.-Y.; Budiawan, W.; Lin, M.-Y.; Lee, C.-H.; Ho, K.-C.; Chu, C.-W. Synergistic Improvements in Stability and Performance of Lead Iodide Perovskite Solar Cells Incorporating Salt Additives. *J. Mater. Chem. A* **2016**, *4*, 1591.

37. Liu, C.; Sun, J.; Tan, W. L.; Lu, J.; Gengenbach, T. R.; McNeill, C. R.; Ge, Z.; Cheng, Y.-B.; Bach, U. Alkali Cation Doping for Improving the Structural Stability of 2D Perovskite in 3D/2D PSCs. *Nano Lett.* **2020**, *20*, 1240.

38. Correa-Baena, J.-P.; Luo, Y.; Brenner, T. M.; Snaider, J.; Sun, S.; Li, X.; Jensen, M. A.; Hartono, N. T. P.; Nienhaus, L.; Wieghold, S.; Poindexter, J. R.; Wang, S.; Meng, Y.; Wang, T.;

Lai, B.; Holt, M. V.; Cai, Z.; Bawendi, M. G.; Huang, L.; Buonassisi, T.; Fenning, D. P. Homogenized Halides and Alkali Cation Segregation in Alloyed Organic-Inorganic Perovskites. *Science* **2019**, *363*, 627.

39. Chen, R.; Hou, D.; Lu, C.; Zhang, J.; Liu, P.; Tian, H.; Zeng, Z.; Xiong, Q.; Hu, Z.; Zhu, Y.; Han, L. Zinc Ion as Effective Film Morphology Controller in Perovskite Solar Cells. *Sustain. Energy Fuels* **2018**, *2*, 1093.

40. Zheng, G.; Zhu, C.; Ma, J.; Zhang, X.; Tang, G.; Li, R.; Chen, Y.; Li, L.; Hu, J.; Hong, J.; Chen, Q.; Gao, X.; Zhou, H. Manipulation of Facet Orientation in Hybrid Perovskite Polycrystalline Films by Cation Cascade. *Nat. Commun.* **2018**, *9*, 2793.

41. Ni, Z.; Bao, C.; Liu, Y.; Jiang, Q.; Wu, W.-Q.; Chen, S.; Dai, X.; Chen, B.; Hartweg, B.; Yu, Z.; Holman, Z.; Huang, J. Resolving Spatial and Energetic Distributions of Trap States in Metal Halide Perovskite Solar Cells. *Science* **2020**, *367*, 1352.

42. Fang, Z.; He, H.; Gan, L.; Li, J.; Ye, Z. Understanding the Role of Lithium Doping in Reducing Nonradiative Loss in Lead Halide Perovskites. *Adv. Sci.* **2018**, *5*, 1800736.

43. Son, D.-Y.; Kim, S.-G.; Seo, J.-Y.; Lee, S.-H.; Shin, H.; Lee, D.; Park, N.-G. Universal Approach Toward Hysteresis-Free Perovskite Solar Cell via Defect Engineering. *J. Am. Chem. Soc.* **2018**, *140*, 1358.

44. Abdi-Jalebi, M.; Andaji-Garmaroudi, Z.; Cacovich, S.; Stavrakas, C.; Philippe, B.; Richter, J. M.; Alsari, M.; Booker, E. P.; Hutter, E. M.; Pearson, A. J.; Lilliu, S.; Savenije, T. J.; Rensmo, H.; Divitini, G.; Ducati, C.; Friend, R. H.; Stranks, S. D. Maximizing and Stabilizing Luminescence from Halide Perovskites with Potassium Passivation. *Nature* **2018**, *555*, 497.

45. Cao, J.; Tao, S. X.; Bobbert, P. A.; Wong, C. P.; Zhao, N. Interstitial Occupancy by Extrinsic Alkali Cations in Perovskites and Its Impact on Ion Migration. *Adv. Mater.* **2018**, *30*, 1707350.

46. Wang, L.; Zhou, H.; Hu, J.; Huang, B.; Sun, M.; Dong, B.; Zheng, G.; Huang, Y.; Chen, Y.; Li, L.; Xu, Z.; Li, N.; Liu, Z.; Chen, Q.; Sun, L.-D.; Yan, C. A Eu^{3+}-Eu^{2+} Ion Redox Shuttle Imparts Operational Durability to Pb-I Perovskite Solar Cells. *Science* **2019**, *363*, 265.

47. Zhao, Y.; Yavuz, I.; Wang, M.; Weber, M. H.; Xu, M.; Lee, J.-H.; Tan, S.; Huang, T.; Meng, D.; Wang, R.; Xue, J.; Lee, S.-J.; Bae, S.-H.; Zhang, A.; Choi, S.-G.; Yin, Y.; Liu, J.; Han, T.-H.; Shi, Y.; Ma, H.; Yang, W.; Xing, Q.; Zhou, Y.; Shi, P.; Wang, S.; Zhang, E.; Bian, J.; Pan, X.; Park, N.-G.; Lee, J.-W.; Yang, Y. Suppressing Ion Migration in Metal Halide Perovskite via Interstitial Doping with a Trace Amount of Multivalent Cations. *Nat. Mater.* **2022**, *21*, 1396.

48. Lu, H.; Liu, Y.; Ahlawat, P.; Mishra, A.; Tress, W. R.; Eickemeyer, F. T.; Yang, Y.; Fu, F.; Wang, Z.; Avalos, C. E.; Carlsen, B. I.; Agarwalla, A.; Zhang, X.; Li, X.; Zhan, Y.; Zakeeruddin, S. M.; Emsley, L.; Rothlisberger, U.; Zheng, L.; Hagfeldt, A.; Gratzel, M. Vapor-Assisted Deposition of Highly Efficient, Stable Black-Phase $FAPbI_3$ Perovskite Solar Cells. *Science* **2020**, *370*, eabb8985.

49. Hui, W.; Chao, L.; Lu, H.; Xia, F.; Wei, Q.; Su, Z.; Niu, T.; Tao, L.; Du, B.; Li, D.; Wang, Y.; Dong, H.; Zuo, S.; Li, B.; Shi, W.; Ran, X.; Li, P.; Zhang, H.; Wu, Z.; Ran, C.; Song, L.; Xing, G.; Gao, X.; Zhang, J.; Xia, Y.; Chen, Y.; Huang, W. Stabilizing Black-Phase Formamidinium Perovskite Formation at Room Temperature and High Humidity. *Science* **2021**, *371*, 1359.

50. Masi, S.; Gualdron-Reyes, A. F.; Mora-Sero, I. Stabilization of Black Perovskite Phase in $FAPbI_3$ and $CsPbI_3$. *ACS Energy Lett.* **2020**, *5*, 1974.

51. Kim, M.; Kim, G.-H.; Lee, T. K.; Choi, I. W.; Choi, H. W.; Jo, Y.; Yoon, Y. J.; Kim, J. W.; Lee, J.; Huh, D.; Lee, H.; Kwak, S. K.; Kim, J. Y.; Kim, D. S. Methylammonium Chloride Induces Intermediate Phase Stabilization for Efficient Perovskite Solar Cells. *Joule* **2019**, *3*, 2179.

52. Xiang, W.; Wang, Z.; Kubicki, D. J.; Tress, W.; Luo, J.; Prochowicz, D.; Akin, S.; Emsley, L.; Zhou, J.; Dietler, G.; Gratzel, M.; Hagfeldt, A. Europium-Doped $CsPbI_2Br$ for Stable and Highly Efficient Inorganic Perovskite Solar Cells. *Joule* **2019**, *3*, 205.

53. Chen, L.; Wu, W.; Wang, J.; Qian, Z.; Liu, R.; Niu, Y.; Chen, Y.; Xie, X.; Zhang, H. Lanthanide Stabilized All-Inorganic $CsPbI_2Br$ Perovskite Solar Cells with Superior Thermal Resistance. *ACS Appl. Energy Mater.* **2021**, *4*, 3037.

54. Fu, S.; Wan, L.; Zhang, W.; Li, X.; Song, W.; Fang, J. Tailoring In Situ Healing and Stabilizing Posttreatment Agent for High-Performance Inverted $CsPbI_3$ Perovskite Solar Cells with Efficiency of 16.67%. *ACS Energy Lett.*, **2020**, *5*, 3314.

55. Liu, D.; Luo, D.; Iqbal, A. N.; Orr, K. W.; Doherty, T. A.; Lu, Z.-H.; Stranks, S. D.; Zhang, W. Strain Analysis and Engineering in Halide Perovskite Photovoltaics. *Nat. Mater.* **2021**, *20*, 1337.

56. Jones, T. W.; Osherov, A.; Alsari, M.; Sponseller, M.; Duck, B. C.; Jung, Y.-K.; Settens, C.; Niroui, F.; Brenes, R.; Stan, C. V.; Li, Y.; Abdi-Jalebi, M.; Tamura, N.; Macdonald, J. E.; Burghammer, M.; Friend, R. H.; Bulovic, V.; Walsh, A.; Wilson, G. J.; Lilliu, S.; Stranks, S. D. Lattice Strain Causes Non-Radiative Losses in Halide Perovskites. *Energy Environ. Sci.* **2019**, *12*, 596.

57. Zhao, J.; Deng, Y.; Wei, H.; Zheng, X.; Yu, Z.; Shao, Y.; Shield, J. E.; Huang, J. Strained Hybrid Perovskite Thin Films and Their Impact on the Intrinsic Stability of Perovskite Solar Cells. *Sci. Adv.* **2017**, *3*, eaao5616.

58. Saidaminov, M. I.; Kim, J.; Jain, A.; Quintero-Bermudez, R.; Tan, H.; Long, G.; Tan, F.; Johnston, A.; Zhao, Y.; Voznyy, O.; Sargent, E. H. Suppression of Atomic Vacancies via Incorporation of Isovalent Small Ions to Increase the Stability of Halide Perovskite Solar Cells in Ambient Air. *Nat. Energy* **2018**, *3*, 648.

59. Zhao, X.; Lu, H.; Fang, W.-H.; Long, R. Correlated Organic–Inorganic Motion Enhances Stability and Charge Carrier Lifetime in Mixed Halide Perovskites. *Nanoscale* **2022**, *14*, 4644.

60. He, C.; Liu, X. The Rise of Halide Perovskite Semiconductors. *Light Sci. Appl.* **2023**, *12*, 15.

61. Li, Y.; Luo, X.; Liu, Y.; Lu, X.; Wu, K. Size- and Composition-Dependent Exciton Spin Relaxation in Lead Halide Perovskite Quantum Dots. *ACS Energy Lett.* **2020**, *5*, 1701.

62. Liang, W.; Li, Y.; Xiang, D.; Han, Y.; Jiang, Q.; Zhang, W.; Wu, K. Efficient Optical Orientation and Slow Spin

Relaxation in Lead-Free $CsSnBr_3$ Perovskite Nanocrystals. *ACS Energy Lett.* **2021**, *6*, 1670.

63. Chen, X.; Lu, H.; Wang, K.; Zhai, Y.; Lunin, V.; Sercel, P. C.; Beard, M. C. Tuning Spin-Polarized Lifetime in Two-Dimensional Metal–Halide Perovskite Through Exciton Binding Energy. *J. Am. Chem. Soc.* **2021**, *143*, 19438.

64. Cheng, H.; Leng, J.; Sun, F.; Zhao, S.; Tang, J.; Wu, K.; Bian, J.; Jin, S. Dopant-Induced Slow Spin Relaxation in $CsPbBr_3$ Perovskite Nanocrystals. *ACS Energy Lett.* **2022**, *7*, 4325.

65. Lin, C.-C.; Liu, T.-R.; Lin, S.-R.; Boopathi, K. M.; Chiang, C.-H.; Tzeng, W.-Y.; Chien, W.-H. C.; Hsu, H.-S.; Luo, C.-W.; Tsai, H.-Y.; Chen, H.-A.; Kuo, P.-C.; Shiue, J.; Chiou, J.-W.; Pong, W.-F.; Chen, C.-C.; Chen, C.-W. Spin-Polarized Photocatalytic CO_2 Reduction of Mn-Doped Perovskite Nanoplates. *J. Am. Chem. Soc.* **2022**, *144*, 15718.

66. Liu, Z.; Qin, X.; Chen, Q.; Jiang, T.; Chen, Q.; Liu, X. Metal–Halide Perovskite Nanocrystal Superlattice: Self-Assembly and Optical Fingerprints. *Adv. Mater.* **2023**, *35*, 2209279.

67. Zheng, B.; Fan, J.; Chen, B.; Qin, X.; Wang, J.; Wang, F.; Deng, R.; Liu, X. Rare-Earth Doping in Nanostructured Inorganic Materials. *Chem. Rev.* **2022**, *122*, 5519.

68. Wang, M.; Lyu, J.; Qin, X.; Yang, S.-W.; Liu, X.; Xu, G. Direct Electron Transfer Enables Highly Efficient Dual Emission Modes of Mn^{2+}-Doped $Cs_2Na_{1-x}Ag_xBiCl_6$ Double Perovskites. *J. Phys. Chem. Lett.* **2022**, *13*, 9429.

69. Zhang, W.; Wei, J.; Gong, Z.; Huang, P.; Xu, J.; Li, R.; Yu, S.; Cheng, X.; Zheng, W.; Chen, X. Unveiling the Excited-State Dynamics of Mn^{2+} in 0D Cs_4PbCl_6 Perovskite Nanocrystals. *Adv. Sci.* **2020**, *7*, 2002210.

70. Han, P.; Luo, C.; Yang, S.; Yang, Y.; Deng, W.; Han, K. All-Inorganic Lead-Free 0D Perovskites by a Doping Strategy to Achieve a PLQY Boost from <2% to 90%. *Angew. Chem. Int. Ed.* **2020**, *132*, 12809.

71. Liu, Z.; Qin, X.; Chen, Q.; Chen, Q.; Jing, Y.; Zhou, Z.; Zhao, Y.; Chen, J.; Liu, X. Highly Stable Lead-Free Perovskite Single Crystals with NIR Emission Beyond 1100 nm. *Adv. Opt. Mater.* **2022**, *10*, 2201254.

72. Qiao, H. W.; Yang, S.; Wang, Y.; Chen, X.; Wen, T. Y.; Tang, L. J.; Cheng, Q.; Hou, Y.; Zhao, H.; Yang, H. G. A Gradient Heterostructure Based on Tolerance Factor in High-performance Perovskite Solar Cells with 0.84 Fill Factor. *Adv. Mater.* **2019**, *31*, 1804217.

73. Xiao, C.; Zhang, F.; Li, Z.; Harvey, S. P.; Chen, X.; Wang, K.; Jiang, C.-S.; Zhu, K.; Al-Jassim, M. Inhomogeneous Doping of Perovskite Materials by Dopants From Hole-Transport Layer. *Matter* **2020**, *2*, 261.

74. Long, G.; Sabatini, R.; Saidaminov, M. I.; Lakhwani, G.; Rasmita, A.; Liu, X.; Sargent, E. H.; Gao, W. Chiral-Perovskite Optoelectronics. *Nat. Rev. Mater.* **2020**, *5*, 423.

75. Ma, J.; Fang, C.; Chen, C.; Jin, L.; Wang, J.; Wang, S.; Tang, J.; Li, D. Chiral 2D Perovskites with a High Degree of Circularly Polarized Photoluminescence. *ACS Nano* **2019**, *13*, 3659.

76. Lyu, K.; Song, E.; Xia, Z. Eu^{2+} Doped Halide Perovskite $KCaCl_3$ with High-Efficiency Blue Emission and Scintillation Application. *J. Mater. Chem. C* **2022**, *10*, 9636.

77. Zhou, Y.; Chen, J.; Bakr, O. M.; Mohammed, O. F. Metal Halide Perovskites for X-Ray Imaging Scintillators and Detectors. *ACS Energy Lett.* **2021**, *6*, 739.

78. Wang, X.; Sun, W.; Shi, H.; Ma, H.; Niu, G.; Li, Y.; Zhi, J.; Yao, X.; Song, Z.; Chen, L.; Li, S.; Yang, G.; Zhou, Z.; He, Y.; Qu, S.; Wu, M.; Zhao, Z.; Yin, C.; Lin, C.; Gao, J.; Li, Q.; Zhen, X.; Li, L.; Chen, X.; Liu, X.; An, Z.; Chen, M.; Huang, W. Organic Phosphorescent Nanoscintillator for Low-Dose X-Ray-Induced Photodynamic Therapy. *Nat. Commun.* **2022**, *13*, 5091.

79. Zhao, H.; Qiu, J.; Hou, B.; Yi, L.; Qin, X.; Liu, X. Flexible Perovskite X-Ray Detectors Through Interfacial Modification with Perylene Diimide. *Adv. Opt. Mater.* **2023**, *11*, 2202668.

80. Hou, B.; Yi, L.; Hu, D.; Luo, Z.; Gao, D.; Li, C.; Xing, B.; Wang, J.-W.; Lee, C. N.; Zhang, R.; Sheng, Z.; Zhou, B.; Liu, X. A Swallowable X-Ray Dosimeter for the Real-Time Monitoring of Radiotherapy. *Nat. Biomed. Eng.* **2023**. https://doi.org/10.1038/s41551-023-01024-2

81. Song, H.; Zhou, D.; Bai, X.; Xu, W.; Dong, B.; Xu, L. Advances in Rare Earth Doped Lead Halide Perovskite Luminescence, Optoelectronic Materials and Devices. *Chinese J. Lumin.* **2023**, *44*, 387.

82. Ding, N.; Wu, Y.; Xu, W.; Lyu, J.; Wang, Y.; Zi, L.; Shao, L.; Sun, R.; Wang, N.; Liu, S.; Zhou, D.; Bai, X.; Zhou, J.; Song, H. A Novel Approach for Designing Efficient Broadband Photodetectors Expanding from Deep Ultraviolet to Near Infrared. *Light Sci. Appl.* **2022**, *11*, 91.